Design of a Ground Static Load Test for a 3 m Joined Wing Flexible Sensorcraft

Francisco Almeida
francisco.maria.a@tecnico.ulisboa.pt

Instituto Superior Técnico, Universidade de Lisboa, Portugal

June 2017

Abstract

Operational requirements for High Altitude, Long Endurance (HALE) aircraft capable of carrying advanced sensor arrays over large territorial areas can be achieved by light weight and geometrically unconventional aerostructures. The Boeing Joined Wing SensorCraft (JWSC) concept is one such example. However, the joined wing configuration presents design challenges due to its non-linear aeroelastic behaviour. Computational models to predict the non-linear aeroelastic behaviour have been developed and reported in the open literature, however experimental data to benchmark analytical predictions is still non-existent. The objective of this thesis is to design a Ground Static Load Test (GSLT), its apparatus and procedures to evaluate the structural response of a flexible joined wing sensorcraft, to understand its static behaviour in terms of displacements, strains and aft wing twist angles when subject to a 2.25g pull-up maneuver. A careful test plan matrix was designed including the appropriate boundary conditions, finite element solvers, ground static test rigs and data acquisition systems. The structural computational model was updated based on the linear deflections. Finally, the validity of the model updating process of a non-linear structure using linear displacements was assessed.
Keywords: sensorcraft, ground static load test, non-linear, finite element model, model update

1. Introduction

The JWSC idea/concept has an aft wing that connects to the front one (usually in a lower position), forming a complex over-constrained system, in a rhombus like form creating thus additional design space and allowing more options in terms of aerodynamics, flight mechanics, engine integration and aero-elasticity [1], [2]. Boeing has a concept of their own and which is a solution proposed to the United States Air Force Research Laboratorys Sensorcraft Request. The aim was to inspire innovation and high-end technology, being the design goal, to integrate the sensing capabilities into an UAV capable of 30 h of endurance at 2000 nm range [3]. The sensorcraft might be seen in figure Being this work embed in the Boeing JWSC project, its purpose relies on designing a GSLT to update the existing FE model based on linear deflections and characterize structure's NL behaviour. Due to the high aspect ratio of this JWSC, very flexible wings (which are made of flexible aluminium spars) are part of the implications. Large deflections will occur and linear assumptions may no longer be valid. The purpose is to provide data and independent analysis of a configuration that demonstrates significant structural non-linearities that aerospace community as a whole, can handle for validation of existing analyses, design tools and methodologies.

Figure 1: Joined wing sensorcraft.

Recent studies carried out by Demasi, *et al* [4] showed how important a NL analysis is when designing a joined wing configuration (in this case, when designing a GSLT for the JWSC). They further concluded that the flexibility of wings and wing joint's connectivity may have a large repercussion on the NL response. A UAV structural demonstrator was developed and used in reference [5] where a static load test was carried out. Globally, the test will have a similar, although more simplified,

approach.

Ifju, *et al* [6] were amongst the first investigators to use Visual Image Correlation technique (VIC) for the full-field basis deformation measurement of rigid and flexible micro aerial vehicles' wings. Galvo, *et al* [7] tried using stereo photogrammetry for displacement measurements of a membrane wing and it was reported a measurement uncertainty of $\pm 35\mu m$ for in-plane measurements and $\pm 40\mu m$ for out-of-plane. Data was available at discrete markers placed throughout the wing. Fleming, *et al* [8] use Projection Moir Interferometry (PMI) which does not demand the use of markers, *i.e.* a fringe pattern is projected onto the wing surface. Displacement's resolution was about 250 μm.

Regarding the update procedure to follow, some work was developed and tested for complex structures which had models to be updated. Its finite element model was divided into substructures, meaning that the design parameters are updated by regions, and proved to be a useful method for large and intricate structural finite element model updating [9].

2. Test Planning

2.1. Preliminary Analyses

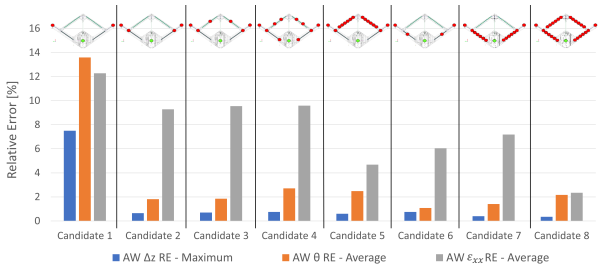

Figure 2: Preliminary analysis quantitative summary.

Several candidates were analysed which account for the different possible options on how and where to apply the concentrated loads. Candidate 1 was the case study to begin with, being the simplest one to carry out on ground. Results were not satisfactory. Candidate 2 allows a big improvement in both displacements and twist angle, being it not as significant for strain. Results stagnate and remain similar for candidates 3 and 4. A small improvement is achieved for candidates 5, 6 and 7. Candidate 8 represents the best case scenario, however with the highest associated complexity. A summary is shown in figure 2. Results are presented as relative errors for the three different measurands considered: displacements (Δz), twist angles (θ) and strains (ε_{xx}). These relative errors calculate de difference between the desired measurand when the sensorcraft undergoes the distributed loads and when it undergoes the equivalent concentrated loads. Candidate 2 was chosen as the one to be used in the GSLT, because it provides a considerably good approximation to the 2.25 g maneuver's deformation with a high simplicity associated.

2.2. Test Rig Preparation

The first step is to determine how the sensorcraft is being tested on ground. As previously said, the goal is to update it through a displacement based on a 2.25 g pull-up maneuver, which is the operational limit. The respective associated loads that the sensorcraft undergoes are known from ASWing interface after simulations are carried out, given the interdependence between structural and aero models. These are complex distributed moments and loads which require simplification to be applied on ground.

The comparable static deformation will be applied using pseudo equivalent punctual loads across the structure. A simple method will be used to determine those loads which consists in constraining (with pin supports only in z direction) the points where punctual loads shall be applied. These constraints are applied in the FE model that is undergoing all the appropriate aerodynamic and inertial loads already known from ASWing, associated to the maneuver. An analysis is carried out with these boundary conditions and the respective reaction forces at each constraint are retrieved, which are the desired simplified loads, only with a single vertical component being then easy to apply experimentally. There are several possibilities on how many loads to use and where to apply it. Eight different cases were tested and the following data represented on figure 3 was elaborated. Each line represents the relative error between the framework undergoing pseudo equivalent and the original complete loads for the quantity in question. In terms of displacement and twist, starting with four loads results become good and for strain, satisfactory.

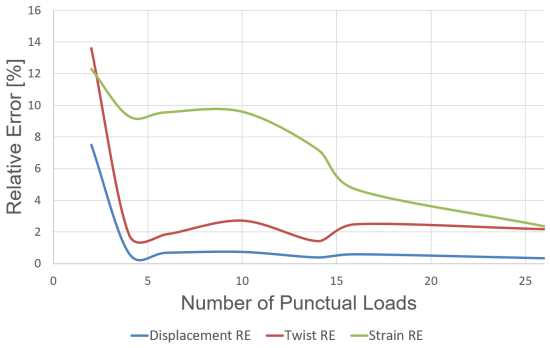

Figure 3: Relative errors achieved for the different number of loads applied.

Aircrafts deformation occurs upwards in aircraft referential. If it is being held to the ceiling, gravity (which is distributed along all the structure) is contributing for deformation as a distributed load and therefore, adding precision to the punctual loads being applied, in the positive flight load direction. Therefore, this will be the set-up of the test. Hence, after several analyses and thoughtful considerations, the best case scenario both in terms of simplicity and acceptable results is having only one load being applied at each side, exactly at the junction between the aft and forward wings, with the sensorcraft being fixed to the ceiling. Final loads are calculated and they are 5.659 kg on each wing.

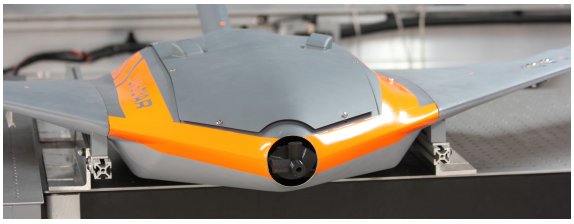

Figure 4: Sensorcraft support rig.

The sensorcraft is being fixed along the interface between fuselage and wings as might be seen in figure 4. These boundary conditions are equally applied between the test and FE model. Loads should be applied with any device which does not damage the structure. The idea found was to have a small sample from a 'T' aluminium extrusion glued to aluminium tape with epoxy. The tape is applied at the desired location onto the respective surface. After some experimental tests, the size of both the tape and the fixture where determined to safely apply the desired loads.

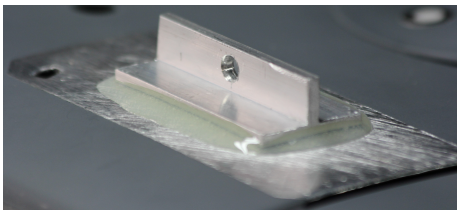

Figure 5: Loads' fixture.

2.3. Data Acquisition System

Displacements were measured by determining the coordinates of certain *a priori* chosen points, using a coordinate measuring machine (CMM). From what was previously done by other researchers and as referred in section 1 the maximum precision achieved was around 0.04 mm and the minimum around 0.25 mm. With the chosen CMM model, the precision annunciated by the manufacturer is 0.1 mm, which is between both precisions already achieved with photogrammetry work. CMM tool will identify predefined targets which will be highlighted with fiducial markers placed on top of sensorcraft's surface. The dots location was chosen based on the criteria that they should be well distributed, along the sensorcraft, which might be then sufficiently represented as the dots are plotted in a 3D graph. Also, they must have a simple correlation with FE models nodes. Strains were measured using conventional foil strain gages. They were placed on top and bottom surfaces of each spar to collect bending strain. Twist angle was measured based on displacement measurements. There are the main points along the wings whose displacements are being measured and further back, auxiliary dots were placed (on the same streamline) so that twist angle along the streamline on those main points might be calculated. Knowing their coordinates the twist angle is automatically determined.

Figure 6: Coordinate measuring machine.

2.4. Testing Procedure

Given the highly non-linear response of the structure, the fact that it will be updated based on linear deformations, and also the troublesome model updating procedure, the static load test and consequent model update will be divided into easier and simpler steps, which are being explained as follows and also presented in figure 7. There are three different FE models which will be updated in chain. These are the individual spars models, the sensorcraft tailless model (with no aft wing) and the complete sensorcraft model. **1:** Spars are individually statically tested, like cantilever beams, with a wide range of loads. **2:** Displacements from one specific load case (within linear range) are measured and introduced in the spars update interface. **3:** Spars FE models are updated based on measured displacements and new stiffnesses are retrieved. Forward spar new Youngs modulus is introduced in the tailless and complete sensorcraft models. Rear spar new Youngs modulus is introduced in the complete sensorcraft FE model. **4:** Tailless sensorcraft is statically tested, with a wide range of loads. **5:** Displacements from one specific linear load case are measured and introduced in the updating tool in-

terface. **6:** FE tailless model is updated based on measured displacements and new stiffnesses are retrieved. which are also introduced in the sensorcraft FE model. **7:** Complete sensorcraft is statically tested, with fractional loads, being the 2.25 g equivalent to the highest load. **8:** Displacements from one specific linear load case are measured and introduced in the FE updating tool. **9:** Sensorcraft FE model is updated based on measured displacements and final stiffnesses are retrieved.

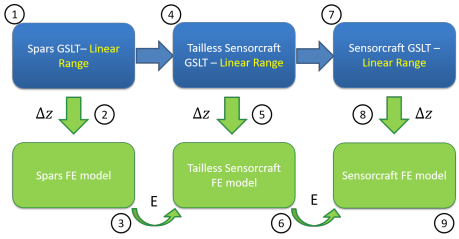

Figure 7: Testing procedure.

2.5. Linear Benchmark

The test to the complete sensorcraft is carried out in steps. Loads are being incrementally applied up to the maximum previously determined. The main objective is to update the FE model based on linear deformations and using a linear solver. The biggest reason behind that is the fact that a linear update is quite less time consuming than doing it using non-linear solver and deformations. Therefore, there is a need to set a benchmark such that the FE model can be updated based on these linear steps. To get a full idea of the linearity of the structure, displacement on the wing tip must be observed and compared to the reference wing span. Estimations were done based on FE simulations. The Linear Benchmark Factor (LBF) is calculated for the following load cases, knowing that half-wing span is 1.5 m and that the displacement is measured at the wing tip:

$$LBF = \frac{\Delta z_{wt}}{1.5} \tag{1}$$

- **Sensorcraft undergoing 10% of the maximum load**. From the FE analysis, it is known that at the wing tip $\Delta z \approx 0.097\ m$, therefore $LBF = \frac{0.097}{1.5} \approx 6.4\%$.
- **Sensorcraft undergoing 5% of the maximum load**. From the FE analysis, it is known that at the wing tip $\Delta z \approx 0.071\ m$, therefore $LBF = \frac{0.071}{1.5} \approx 4.7\%$.

As calculated, for the 10% load factor to be applied to the sensorcraft, the validity of linearity is not safe to be assumed as such. Hence, **sensorcraft's deformation when undergoing 5% load factor might still be considered linear, considering that the displacement up to 5% of the reference wing span (LBF previously calculated) may be considered negligible**. Thus, a linear solver may then be used to analyse the FE model, in those circumstances. Also, the linear update might be based on smaller deflections originated from small load factors.

3. Results

The model was updated based on stiffnesses only. This is due to the fact that geometries were not desired to be changed or remodelled, because the FE structural model has a direct influence on the ASWing aero framework. The update procedure is carried out using Dynamic Design Solutions FEMtools software.

Regarding spars' test, results are presented in figures 8 and 9, where it is observable the deformation at each load step applied and a plot for displacement at the farthest lengthwise measurement point for each applied load. As it is clearly observable, experimental data is unquestionably close to the one retrieved from the FE non-linear solver. The predictable non-linearity for the behaviour, given the large deflections, is confirmed in the spars themselves, and the FE NL solver keeps up well with reality.

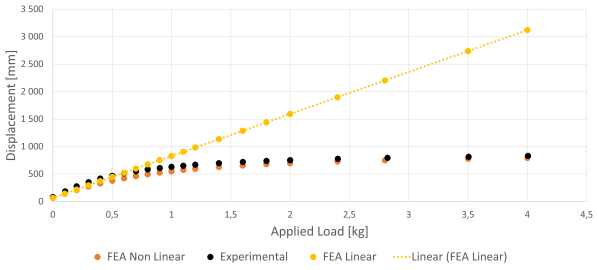

Figure 8: Aft spar test results.

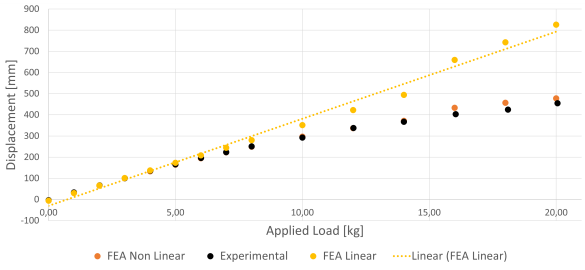

Figure 9: Forward spar test results.

There are different groups of elements within the FE model that intend to represent the several logical different sections of the real aircraft. It was updated globally which is the update procedure based on changing the stiffnesses of those groups in order

to achieve the desired displacements. All elements within a group have the same properties. Therefore, a global parameter represents a coincidental change of physical properties of a set of nodes/elements. These different groups can be seen in figure 10.

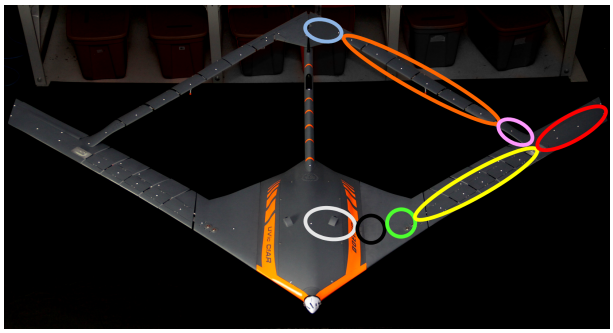

Figure 10: Sensorcraft update groups.

Table 1 presents the tests carried out for the tailless and complete sensorcrafts.

Test	Clamping	Loads Undergone
1	Table	Gravity
2	Ceiling	Gravity
3	Ceiling	Gravity + 5% of Max Load
4	Ceiling	Gravity + 10% of Max Load
5	Ceiling	Gravity + 20% of Max Load
6	Ceiling	Gravity + 40% of Max Load
7	Ceiling	Gravity + 60% of Max Load
8	Ceiling	Gravity + 80% of Max Load
9	Ceiling	Gravity + 100% of Max Load
11	Table	Gravity
12	Ceiling	Gravity
13	Ceiling	Gravity + 5% of Max Load
14	Ceiling	Gravity + 10% of Max Load
15	Ceiling	Gravity + 20% of Max Load
16	Ceiling	Gravity + 40% of Max Load

Table 1: Experimental tests.

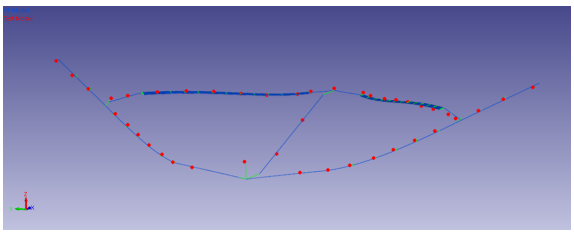

Figure 11: Complete model experimental and FE data.

A picture of the tests carried out for the sensorcraft is presented.

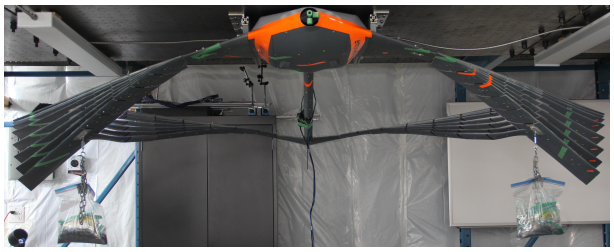

Figure 12: Complete sensorcraft test.

Some examples of the obtained results are next presented in the following figures, where it is possible to observe the improvement achieved with the update done to the framework. Regarding the plots, the darker green line represents the obtained linear FE solution whereas the light green one shows the non-linear FE results. This example shows how important the non-linear solver is for this kind of framework. The blue line represents the experimental twist angle and the thinner red line accounts for the relative error between the light green and blue lines.

It is important to understand how well the update procedure (done with linear displacements) extrapolates to the maximum displacement non-linear case. Therefore results are shown for the maximum load case, equivalent to the desired 2.25 g pull-up maneuver. The first two figures present displacement for the aft wing. Figure 13 shows that there is a slight difference between linear and non-linear solvers and, it is possible to see how the latter is the closest to the experimental results. Neglecting the peak happening at the root, the error is around 35% for the left side and 20% for the right one. On the other hand, figure 14 demonstrates that displacements are considerably better, being the error now around 18%. However, it does not have the ideal shape, which was impossible to achieve without causing a dramatic change in either twist or strain, being this the best achieved result for the several different options tried. The FE aft wing does not buckle as much as the as-built one. This fact might also be due to the way the spar was geometrically modelled.

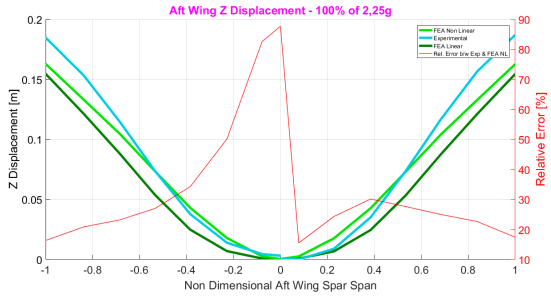

Figure 13: Aft wing's original displacement.

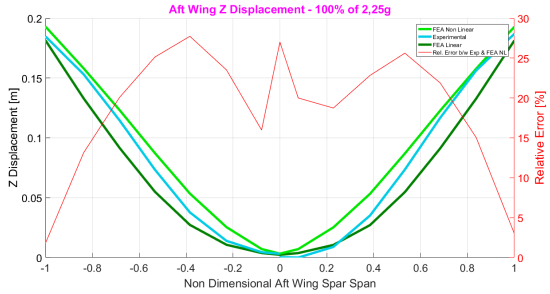

Figure 14: Aft wing's updated displacement.

The second group of pictures presents forward wing displacements. Figure 15 shows that the relative error is around 15%. Besides, the linear solution method proves to be still a good approach, which demonstrates that even with a load of this magnitude and high displacement, forward wing's behaviour might be well reproduced by means of a linear solver. Experimental and FE non-linear results match almost perfectly in figure 16. The relative error between both drops to an average of 4%, which is a really good result. The plot for Δ_z along wings span shows how the light blue and light green lines are almost overlaid.

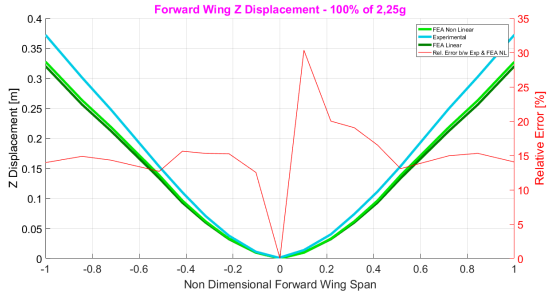

Figure 15: Forward wing's original displacement.

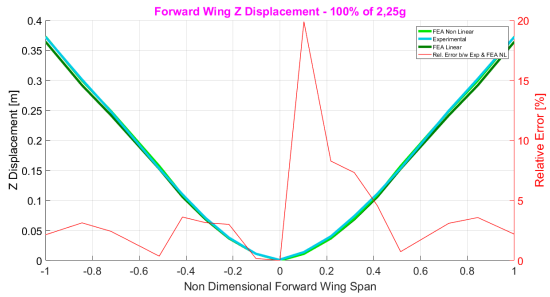

Figure 16: Forward wing's updated displacement.

The fifth and sixth plots illustrate strain on the aft wing. The trend for the FE analysis non-linear ε_{xx} shown in figure 17 is similar to the one observed experimentally, however results are off by around 100%, this is explained by the fact that strain is being taken out of the computational model in the edges of the plate elements. Given the way the aft spar was modelled, this was the only place equivalent to where strains are measured experimentally. Therefore, results are already expected to be considerably off in terms of magnitude, however the trend is similar, which is important. Strain presents well why a linear solution method is not advisable for such a flexible structure It clearly does not follow the experimental trend. Figure 18 shows that the shape was corrected and it is now similar to the experimental measured one, although with a considerable difference in magnitude. Once more, the huge error is due to the lack of accuracy of the model as far as strains is concerned, in the aft wing.

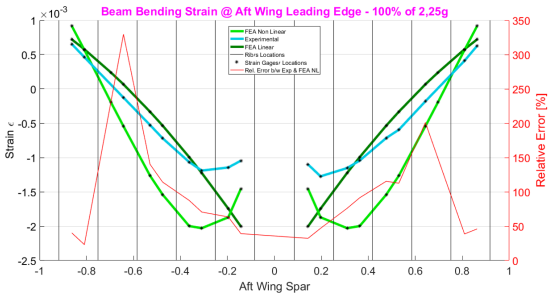

Figure 17: Aft wing's original strain.

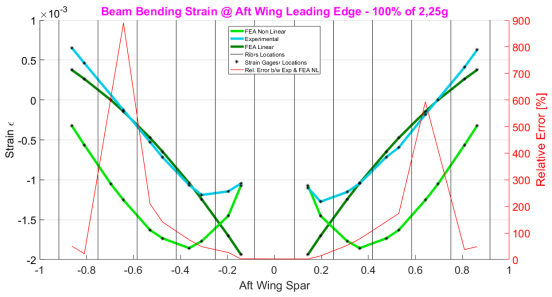

Figure 18: Aft wing's updated strain.

The last set o graphs present the twist angle along both aft wings. θ data presented in figure 19 strengthens more the fact that linear and non-linear analysis have totally different results and this is where an appropriate non-linear solution method becomes important. The twist relative error between FE and experimental is around 25%. Figure 20 shows that twist was also improved, having now an error of around 13%.

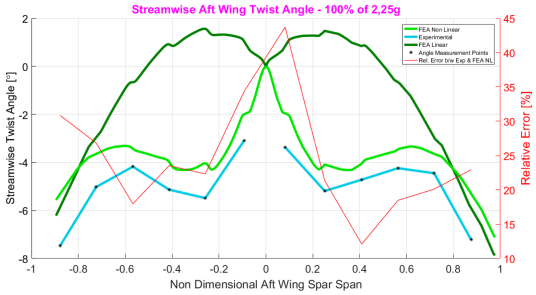

Figure 19: Aft wing's original twist angle.

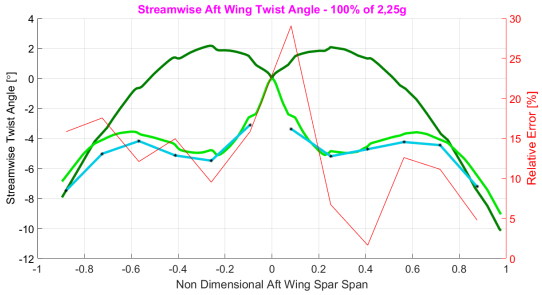

Figure 20: Aft wing's updated twist angle.

The FE model is now more flexible, displacing and twisting more, accordingly to the as-built aircraft. Both twist and strain, in this case, show how important it is to approach this problem with an accurate non-linear solver, being the difference between linear and non-linear solutions hugely different. Being the sensorcraft updated based on measured displacements, it was expected for this measurand to be the most precise one, which could provide a better insight over the update procedure, *i.e.* FE models Youngs moduli were updated using the measured displacements, and for the sake of the update procedure itself, this is the only quantity that can tell if the update procedure was successful. Although the good improvement achieved for both strain and twist, they are not a major fact when assessing the feasibility of the update procedure. Table 2 presents a summary of relative errors (RE) between FE solutions and experimental results, for all quantities measured throughout the process: displacement in the vertical direction (Δz), bending strain (ε) and twist angle along stream line (θ). 'F' accounts for the forward wing and 'A' for the aft one. On the left side, results are presented for the 5% load case (the one used for the update procedure), and on right side the maximum load case is shown.

4. Conclusions

The goal was to understand the behaviour of the structure when undergoing significant loads, that induced a non-linear response of the structure in terms of the twist angle on the aft wing. The significant conclusions from this research can be summarized as follows:

		5% RE [%]		100% RE [%]	
		Initial	Updated	Initial	Updated
F	Δz	14.5	4.1	16.2	4.3
	ε	30	18.3	18.1	7
	θ	28.1	10.1	26.2	5
A	Δz	32.4	15.9	30.1	18
	ε	64.3	53.6	92.8	145.6
	θ	71.7	50.1	24.3	12.7

Table 2: Results summary.

- The MSC Nastran 400 non-linear solution method provided results that agreed well with the experimental data.
- The aft wing presents clear evidence of non-linear behaviour. If the forward wing is being considered alone, a linear solver might still be accurate, however considering also the existence of the aft wing, a non-linear solver must necessarily be used.
- Overall, a reduction of more than half the original error between experimental and computational results was achieved. For the maximum load case, the average error is around 10% for all measurands (excluding strain in the aft wing).
- It was found that the aft wing spar geometric modelling is inadequate, in terms of strain measurement, for this specific case. A new modelling is suggested, either with CQUAD elements in a different layout or using 3D elements instead, as it might be seen ahead.
- Experimental static test procedure proved to be successful and an adequate approach to update the finite element model of the non-linear aerostructure.

4.1. Future Work

The initial model was built with the purpose of being simple and parametric and easily adjusted for development of a design space, to better understand sensorcrafts behaviour. It was arguably a good approximation, from what static load test results tell. However, improvements could be carried out as follows:

- Some joints are modelled as rigid elements, not allowing then as much freedom for the update

procedure as it could. Also, the freedom of different sections against each others becomes compromised. A joint parametrisation for the several interfaces within the structure would be an improvement. These main interfaces are the forward wing with the fuselage, the aft wing with the boom and the forward wing with the aft wing.

- Adapting the aft wing to better represent the interfaces where it was decided to measure strain from, *i.e.* to remodel its geometry and constituent elements. Some suggestions are given:

  - The simplest way of remodelling would be to maintain the plate elements, although changing their position so that strain could be measured in the middle of the surface and not in the edge. This solution might be seen in figure 22.

  - Aft spar could have a hybrid modelling with 2D shell and 3D solid elements. For instance, the same modelling with horizontal shell elements in the middle section could be kept, with the two protuberances being changed to 3D solid elements. Hence, strain would be measured in the side of a solid element. This can be seen in figure 23.

  - Lastly, aft spar could be integrally modelled with solid 3D elements, reliably recreating the as-built spar, as represented in figure 24.

Figure 21: Original modelling.

Figure 22: 2D elements alternative modelling.

Figure 23: Hybrid elements alternative modelling.

Figure 24: 3D elements alternative modelling.

Acknowledgements

I would like to thank the team whose help was crucial throughout the development of this work at the Centre for Aerospace Research in Victoria, specially Dr. Afzal Suleman for making this possible. This work would never have been accomplished without a team like this behind.

References

[1] J. Richards. An Experimental Investigation of a Joined Wing Aircraft Configuration Using Flexible, Reduced Scale Flight Test Vehicles. Ph.D. Dissertation, University of Victoria, 2009.

[2] R. Cavallaro and L. Demasi. Challenges, Ideas, and Innovations of Joined-Wing Configurations: A Concept from the Past, an Opportunity for the Future. In *Progress in Aerospace Sciences*, 87 pages 1–93, 2016.

[3] D. Lucia. The SensorCraft Configurations: A Non-Linear AeroServoElastic Challenge for Aviation. In *Structural Dynamics and Materials Conference* Austin, 2005.

[4] L. Demasi, R. Cavallaro, and F. Bertuccelli. Post-critical Analysis of Highly Deformable Joined Wings: The Concept of Snap-divergence as a Characterization of the Instability. In *Journalof Fluids and Structures*, volume 54, pages 701–718. Apr. 2015.

[5] G. Frulla and E. Cestino. Design, Manufacturing and Testing of a HALE-UAV Structural Demonstrator. In *Composite Strcutures*, volume 83, pages 143–153. 2007.

[6] P. Ifju, R. Albertani, B. Stanford, D. Claxton, M. Sytsma. Flexible-Wing Micro Air Vehicles. In *Introduction to the Design of Fixed Wing Micro Air Vehicles*, chapter 5, AIAA, 2015.

[7] R. Galvao, E. Israeli, A. Song, X. Tian, K. Bishop, S. Swartz and K. Breuer. The Aerodynamics of Compliant Membrane Wings Modeled on Mammalian Flight Mechanics. In *AIAA Fluid Dynamics Conference and Exhibit*, San Francisco, Jun. 2006.

[8] G. Fleming, S. Bartram, M. Waszak, and L. Jenkins. Projection Moire Interferometry Measurements of Micro Air Vehicle Wings. In *SPIE International Symposium on Optical Science and Technology* National Aeronautics and Space Administration, 2001.

[9] T. Marwala. Finite Element Model Updating Using Computational Intelligence Techniques-Applications to Structural Dynamics. In *Springer-Verlag* 2010.